THE STRUCTURE OF THE THERMOSPHERE AND ITS VARIATIONS

by

Isadore Harris
Goddard Space Flight Center, NASA
Greenbelt, Maryland

and

Wolfgang Priester
Astronomische Inst~~itute~~ der Universität Bonn
Bonn, Germany

and

Institute for Space Studies
Goddard Space Flight Center, NASA
New York, New York

10/67

ABSTRACT

The diurnal variation of the thermosphere is the key feature for a theoretical understanding of the entire thermospheric structure and of its energy balance (heating processes, heat loss, conduction and convection). The earlier attempts (in 1962) in calculating the diurnal variation failed to yield the diurnal maximum of density and temperature at the observed time of 1400 hours. In these attempts no horizontal interaction was included. The recent calculations of the horizontal wind system, which is set up by the pressure gradients of the atmospheric bulge, showed that winds in the order of 100 to 200 m/s in the altitude range from 200 to 400 Km can provide a large horizontal energy transport. It cannot be decided yet whether the horizontal advection alone is sufficient to remove the whole discrepancy between the calculated time of the diurnal maximum (1700 hours local time) and the observed time (1400 hours).

Recent considerations on anomalous heat conduction through the magnetosphere have some bearing on the question whether the upper thermosphere is fully isothermal. This is important for the calculations of the diurnal variation since even a small temperature gradient at the thermopause can have a non-negligible effect, in particular, if the temperature gradient varies with local time.

1. Introduction

In the course of the past ten years a detailed picture of the structure of the thermosphere and lower exosphere has emerged from satellite and rocket measurements. In particular, the vast number of measurements of the drag exerted by the atmospheric atoms and molecules on the satellite has revealed five different effects which cause variations of density and temperature of the neutral gas. Furthermore, the data have provided some insight into the dependence of atmospheric properties on latitude and season. In this brief review we shall restrict ourselves to a height range of 100 Km to 1200 Km, where most of the satellite-and high-altitude-rocket-measurements were made.

The 5 effects are:

1) the diurnal variation ("atmospheric bulge")
2) the solar activity effect (27-day-variation)
3) the solar cycle effect (11-year-variation)
4) the geomagnetic activity effect
5) the semiannual variation.

For detailed information we refer to a recent review by W. Priester, M. Roemer and H. Volland (1967) and in particular, for new results on the seasonal-latitudinal variations to papers by L. G. Jacchia and J. Slowey (1967) and G. M. Keating and E. F. Prior (1967). Furthermore a detailed review on the observational results of satellite drag analysis was given by L. G. Jacchia at the IQSY/COSPAR Symposium 1967 at London (to be published in the Proceedings of the IQSY. In this paper we shall only give a few illustrations to some of the aforementioned effects. A satellite which nicely displayed the diurnal variation and the geomagnetic activity effect superposed on it was Injun III. L. G. Jacchia and J. Slowey (1963) determined from the drag-induced acceleration of this satellite the atmospheric density at an altitude of 250 Km (corresponding to the perigee altitude) for the time from December 15, 1962 through June 29, 1963. These data are given in the lower part of Fig. 1. During the observational period the local time of the satellite's perigee passed twice through the 24-hours. The local time is given as the lower x-axis of Fig. 1. On the top the dates of observation are given in the usual scale and in modified Julian dates (MJD). The solid and the dotted curves represent the corresponding theoretical density values (from Harris and Priester 1962b) for the 1963 prevailing levels of solar activity marked S = 90 and S = 100. The histograms in the upper part give the daily geomagnetic indices A_p and the solar 10.7 cm flux F. The black dots represent the densities during geomagnetically quiet days ($A_p \leq 2$). These data should be compared with the theoretical curves. There are, however, no corrections made for either the correlation of the density with the 10.7 cm flux ("solar activity effect") nor for the semi-annual variation. The latter shows up as low density values in December 1962, January 1963 and in June 1963. The most remarkable feature of Fig. 1, however, is the strong response of the density to geomagnetic storms.

The quiet-day diurnal density variation of 250 Km in 1963 has an amplitude of a factor of 1.9. For years of high solar activity, for instance in 1958/1959 the amplitude was much smaller. This is borne out in Fig. 2, which gives the density distribution in the height range from 200 to 700 Km for diurnal maximum (1400 hours local time) and diurnal minimum (0400 hours local time) for two levels of solar activity (Fig. 2 is taken from CIRA 1965). The high activity is represented by a 10.7 cm flux $\overline{F}$ = 200, the low activity by $\overline{F}$ = 75. It is remarkable, that the entire variation of the density at a height of 600 Km exceeds two orders of magnitude during the eleven-year solar cycle.

As an example of the semi-annual variation we used the recent results obtained by G. E. Cook and D. W. Scott (1966) from the satellite Echo 2 during 1964 and 1965. These data show how strong the effect is at an altitude of 1130 Km for the rather low level of solar activity in 1964, 1965 (Fig. 3). It also shows that the June, July minimum is lower, as usually observed, as the January minimum. In 1965 the summer minimum is misplaced due to a rather strong continuous increase of the solar activity level during June, July 1965 which masks the semi-annual minimum. There is no satisfactory theoretical explanation yet for the semi-annual variation.

The recent investigations of high-inclination satellites have revealed more information on the dependence of density and temperature on latitude and season, which proved that the bulge center for altitudes below 600 Km follows the seasonal changes of the declination of the sun (Jacchia and Slowey (1967)). For altitudes above 600 Km, where helium is supposedly the dominant constituent of the neutral gas for periods of moderately low solar activity, the density was found to be largest on the winter hemisphere at high latitudes. This was termed the "winter helium bulge" by Keating and Prior (1967). The finding of this surprising behavior of the density was also confirmed by Jacchia and Slowey (1967).

2. The structure of the thermosphere

The basic feature of the thermosphere is the very steep increase of the temperature with height in the altitude range from 100 to 200 Km and the leveling-off of the temperature curve in the upper thermosphere (200 to 500 Km).

The steep temperature gradient is caused by the heating derived from the absorption of the solar XUV radiation, in particular, in the wavelength range from 100 to 912 Å which was repeatedly measured by H. E. Hinteregger and his collaborators (see: Hinteregger et al., Space Rec. V 1965). This part of the solar spectrum originates primarily (or at least to 50 percent) in the solar corona-condensations above sunspot areas. This became evident when the early observations of satellite orbital periods (Jacchia 1958) revealed time-variations of the atmospheric drag, indicating variations in density and temperature in the thermosphere, and when it was found that these variations correlate with the solar decimeter flux (Priester 1959). From the theory by M. Waldmeier and H. Mueller (1950) it was known that the so-called slowly varying component of the solar decimeter radiation originates in the coronal condensations. The correlation with thermospheric parameters then revealed immediately that the XUV radiation also mostly originates in the condensations, due to the rather close correlation to be expected on theoretical grounds between the decimeter and the XUV flux. It furthermore proved that the XUV absorption is responsible for most of the heating of the thermosphere. Later in 1962 the observations with OSO I confirmed that the integrated XUV flux and the 10.7 cm radiation were proportional to each other.

For altitudes above 200 Km the increasing mean free paths of the neutral air molecules and atoms cause a rapid increase of the heat conductivity which in turn must lead to an isothermal structure in the upper thermosphere provided that there is no appreciable heat influx from above, for instance by heat conduction through the magnetosphere. This general structure was pointed out as early as 1951 by D. R. Bates (1951) (see also M. Nicolet (1961), F. S. Johnson (1958)).

That the temperature of the isothermal part of the upper thermosphere undergoes a large diurnal variation of several hundred degrees Kelvin came to light only when the large diurnal variation in density was discovered from the analysis of drag data by L. G. Jacchia (1959), S. P. Wyatt (1959) and W. Priester and H. A. Martin (1960) independently of each other.

3) The diurnal variation of the thermosphere

The diurnal variation of density and temperature has been observed in the height range from 200 to 800 Km showing a steep increase in the morning, a maximum at 1400 hours local time, followed by a steep decline during the afternoon and a considerably less steep decline during the night with a minimum at about 0400 hours local time. These observations pertain to equatorial and moderate latitudes.

The effect is caused by the heating due to absorption of solar energy and by the heat conduction of the neutral gas which conducts the energy down into the mesopause (85 Km) where it will be mostly eliminated from the atmospheric energy balance by reradiation processes.

Attempts have been made to calculate the diurnal behavior of the thermosphere by Harris and Priester (1962a, 1962b, 1963a, 1963b, 1965) and in a slightly different way by Mahoney (1966).

A completely satisfactory solution can only be expected if one solves the following set of hydrodynamic and thermodynamic equations for the spherical earth:

$$\frac{\partial \rho}{\partial t} + \mathrm{div}\,(\rho \vec{v}) = 0$$

(conservation of mass),

$$\rho \frac{\partial \vec{v}}{\partial t} + \mathrm{grad}\; p + \mathrm{Div}\; \sigma + \rho \vec{g} = 0$$

(conservation of momentum),

$$\rho c_v \frac{\partial T}{\partial t} - \mathrm{div}\left(K\, \mathrm{grad}\, T\right) + p\; \mathrm{div}\; \vec{v} = q \tag{1}$$

(conservation of energy),

$$p = \frac{R}{M} \rho T$$

(ideal gas equation),

with the five unknowns density ρ, pressure p, temperature T and the components u, v, and w of the wind velocity $\vec{v} = \vec{v}(u,v,w)$. $\vec{g}$ is the gravitational acceleration, σ is the viscous stress tensor, c_v is the specific heat at constant volume, K is the coefficient of heat conductivity and q contains the solar heat flux and the heat loss due to infrared reradiation of the atmosphere.

Due to limitations of computer capacity and unknown boundary conditions, in particular of the wind systems, Harris and Priester (1962), following an earlier procedure by R. Jastrow and L. Kyle reduced the system in such a way that it depends on height and time only for the latitudinal range of the equator. This implied the assumption that horizontal energy transport by winds was of minor importance. Nowadays this assumption can be no longer maintained. Nevertheless the simplified calculations provided useful insight into the energy balance of the thermosphere.

The calculations were based on the following premises:

1) Hydrostatic equilibrium is reached sufficiently rapidly at all heights and times.

2) Diffusive equilibrium holds in the entire range from 120 to 1000 Km.

3) The boundary conditions at 120 Km (number densities of N_2, O_2, O, A, He, H and the temperature) do not vary with time. This condition, however, was abandoned in later versions of the investigation (Harris and Priester 1965, and as yet unpublished calculations in 1966 and 1967) in order to study the effects of time-dependent boundary conditions.

4) Heat flow was permitted only in the vertical direction - no lateral conduction or advection. This condition, again, was eased, when the effects of lateral conduction and convection in the equatorial plane were investigated.

As a heat source the absorption of the solar XUV-radiation in the range from 100 to 1000 A was used with average values for the absorption cross sections of N_2, O_2 and O. It was proved that taking average values for the cross sections over the entire wavelength range did not alter the height distribution of heat in any significant way. This proof was done by splitting the total range into five wavelength ranges with the corresponding cross sections. Also the investigation by Mahoney (1966) who used 32 ranges of wavelength and the corresponding cross sections showed no significant differences in the resulting atmospheric parameters as compared to the calculations with one average cross section for each of the three main constituents.

The heat conversion coefficient was taken to be 37 percent and independent of height and the chemical composition of the atmosphere. In our 1965 calculations we also added the heat provided by absorption of the radiation in the Schumann-Runge range (1300-1700A). This, however, has only an effect on the magnitude of the temperature gradient at the lower boundary (120 Km), but does not significantly influence the diurnal behavior of the thermosphere.

Furthermore, the heat loss by reradiation from oxygen atoms was taken into account. As D. R. Bates (1951) had shown, only the radiation emitted by the transition from the $^3P_1$ to the $^3P_2$ level of atomic oxygen is important. In general the amount of energy radiated away by this process is less than 10 percent of the absorbed XUV flux. Only close to the lower boundary altitude (120 Km) does the emitted radiation become comparable to the absorbed amount of the XUV radiation.

The solution of the time-dependent heat conduction equation in connection with the formulae for diffusive equilibrium and using the heat sources explained above did not yield a satisfacotry agreement between the observed and the calculated densities and temperatures. For the latter we should bear in mind that the temperatures could not be observed directly in the upper thermosphere. But it is believed that the temperatures inferred from the observed densities are accurate to within a limit of about 20 percent.

A more detailed mathematical description of this result and the comparison between observed and calculated atmospheric parameters can be found in SPACE RESEARCH III (Harris and Priester, 1963a). An illustration of the discrepancy is given in Fig. 4. The curve T_M represents the "observed" temperatures, the curve T_{EUV} represents the calculated diurnal temperature variation in the upper thermosphere. (The curve T_C will be discussed in a later chapter of this paper.) The temperatures correspond to a rather high level of solar activity, characterized by a 10.7 cm solar flux of $\overline{F} = 200$ flux units (10^{-22} W/m^2 Hz). The total range of solar activity within the eleven-year cycle ranges from above $\overline{F} = 250$ down to $\overline{F} = 60$.

From Fig. 4 we conclude that within the frame of the outlined theory an agreement between observations and theory cannot be obtained because the calculated maximum occurs at about 1700 hours instead of 1400 where it is observed. Furthermore, the requirements for the efficiency of conversion of absorbed solar XUV radiation into heat were prohibitively large. The total amount of flux required for conversion into heat was 2.5 erg/cm^{2}sec. This was the amount which had been measured by H. E. Hinteregger (1961). Thus apparently the requirement is a 100 percent conversion efficiency, which is unacceptable. Later on the situation regarding the absolute flux values eased somewhat due to improved measurements which pertain to lower levels of solar activity. While the measured flux values remained practically the same, the amount of heat required in the theory decreased proportionally to the decreasing solar 10.7 cm flux. Since, however, the observed behavior of the upper atmosphere during the entire decreasing phase of solar activity from 1958 through 1963 rather conclusively requires that the XUV flux should vary in proportion to the 10.7 cm flux it is believed that the earlier measurements of the flux yielded values considerably too small. We shall have to wait for the next solar maximum for new measurements of the XUV flux in order to reach final conclusions on the problem.

In Fig. 5 the diurnal distribution of the heat sources integrated over the entire height range is given. These integrals correspond to the amount of solar flux available for the heating of the thermosphere. The curve labeled No. 4 with a total flux of 2.5 erg/cm^2 sec would yield the curve T_{EUV} in Fig. 4 with the maximum late by 3 hours. The curve No. 3 is made in such a way as to yield agreement with the observed data (curve T_M in Fig. 4). In 1962 it was concluded from the then available measurements that the amount of XUV flux available for heating was only in the order of 1 erg/cm^2 sec (under the assumption of a conversion efficiency of 37 percent). This is represented by the dotted curve No. 1. Since this flux was highly insufficient we concluded in 1962 that there should be a "second heat source". The second heat source required for agreement between observation and theory is given by curve No. 2 in Fig. 5. The curves 1 and 2 together yield curve 3. In 1962 it was believed that the discrepancy in the energy required could be provided by the solar wind. This idea was stimulated by the fact that during geomagnetic storms a considerable heating of the thermosphere takes place, the energy of which derives from the solar wind.

In the light of the situation with regard to the direct flux measurements it is now the preferred theory that there might be as much flux available for heating as indicated by curve 4 for a solar activity level of F = 200. In order to shift the energy into curve 3 a horizontal transport mechanism is required. This mechanism is sought in a global horizontal advective flow pattern, which is set up by the pressure gradients between the maximum and the minimum of the diurnal atmospheric bulge. The curves 3 and 4 are made in such a way that the areas underneath the curves are the same. Thus they both provide the same amount of total energy.

4. The effect of a global wind pattern on the diurnal variation

A few years ago the wind speeds which might occur in the thermosphere were usually grossly underestimated. Then, from artificial cloud release measurements and from theoretical considerations, it became more and more obvious that winds with speeds exceeding 100 m/s might occur in the thermosphere and that the diurnal bulge ought to generate a global wind system with speeds in the same range.

Wind patterns have been derived from the pressure gradients of the diurnal bulge by R. S. Lindzen (1966), J. E. Geissler (1966, 1967), H. Kohl and J. W. King (1966), H. Kohl (1967) and by I. Harris (1966).

I. Harris also investigated the effect of the horizontal winds on the shape of the diurnal temperature and density distribution. Since the available computer capacity was insufficient for a full treatment of the winds on a spherical earth, he restricted the computations to the equatorial plane. But these calculations are the only ones from the references mentioned above which include non-linear inertial terms. Due to the restriction to the equatorial plane the resulting corrections on the diurnal variation can only be regarded as indicative of the order of magnitude of the effect at the different hours of the day. Nevertheless, it yields some valuable insight into the more comprehensive problem.

Within the computations of the winds there remained one problem which is not yet fully explored. That is the question of the effectiveness of the ion drag which prevents the neutrals from flowing freely. In particular, in the equatorial plane the ions will be rather effective in reducing the wind velocity of the neutrals in longitudinal directions, since the ions can be regarded as essentially fixed on the magnetic field lines of the earth, which is basically perpendicular to the equatorial plane. In his calculations I. Harris used for the number densities of the ions the electron density profiles as given by S. Chandra (1963) for daytime and nighttime conditions. He further applied S. Chapman's (1956) expression for the collision frequency between the neutrals and the ions and assumed an average of half the momentum transferred in each collision. Under these assumptions the calculated wind velocities in the equatorial plane remained rather small and therefore had no significant effect on the diurnal temperature distribution.

In order to see under what circumstances the wind system would be effective enough to provide the appropriate shift in the diurnal curve, the effect of the ion drag was reduced artificially in the computations. But only when the ion drag was reduced to 10 percent of its original value as represented by the above stated assumptions the wind speeds reached values as high as 200 m/sec at an altitude of 300 Km. The thus obtained velocity distribution in the equatorial plane is given in Fig. 6. The basic feature is an East to West wind in the morning and a West to East wind in the late evening.

The effect of this wind system on the diurnal temperature curve is shown by the solid curve labeled T_c in Fig. 4. We can see that the horizontal advection has reduced the amplitude of the diurnal temperature variation considerably. It also shifted the entire curve to earlier hours of local time. There remained, however, a rather curious maximum close to 1600 hours. Since it cannot be expected to have any better agreement between "observed" and calculated temperatures due to the simplifications in the calculations, in particular the restriction to the equatorial plane, it must be concluded that a global wind system can provide the required shift of the atmospheric bulge center to a time of approximately 1400 hours local time, provided that the ion drag does not effectively prevent high winds from occurring. Of course, the ion drag effect will be maximum in the equatorial plane and will be much less preventive in the other directions.

5. Limitations of the thermospheric models

A remarkable feature of the satellite drag measurements is the large reliability of the correlation of atmospheric parameters with solar and geomagnetic activity and the stability of the atmospheric bulge, the maximum of which remains close to 1400 hours local time throughout the solar cycle (so far established for the seven-year period from solar maximum through solar minimum only). We have to bear in mind, however, that satellite drag results provide density data, which are averaged over a considerable range in time and distance. Therefore in any comparisons of the models' predictions with instantaneous measurements some caution must be exercized. This is particularly suggested by the larger scatter of direct measurements and by the recent discovery of two different wave phenomena. One type was found in the lower thermosphere by K. Mauersberger et al. (1967), the other kind in the upper thermosphere by G. Newton et al. (1967).

Another important aspect of the theoretical calculations of the thermospheric behavior is the constancy of the boundary conditions at both the lower and the upper height limit, usually taken at 120 Km and at about 1000 Km. The choice of the height of the upper boundary is rather unimportant. It can be selected anywhere between 500 and 1000 Km without any significant influence on the thermospheric structure.

Time-dependent variations of the boundary conditions can, however, be important. Diurnal variations of the density and temperature at a height of 120 Km are believed to remain rather small with a temperature change confined in a range of less than 10^{0}K. If so, this will alter the numerical values of atmospheric model parameters, but is not apt to influence the concept of the physical processes involved.

At the upper boundary usually only a value of the temperature gradient is assumed; mostly taken to be zero because of the supposedly very effective insulation of the thermosphere from the solar wind by the magnetosphere. Recently, however, it has become more and more apparent, that in the rather unstable plasma of the magnetosphere the ionic heat conduction perpendicular to the magnetic field lines, might be greatly enhanced at the expense of the conductivity parallel to the field lines, with the effect that the "perpendicular" conduction could reach nearly the same order of magnitude as the "parallel" conduction (T. Tsuda (1967), W. Priester, M. Roemer and H. Volland (1967), H. G. Mayr and H. Volland (1967)). If this is so, it might distort the isothermal structure of the neutral gas in the lower exosphere, yielding a temperature gradient in the order of 1 ^{0}K/km at heights of about 800 Km.

In this context it is worthwhile to look at the entire temperature structure and also at the deviations from thermal equilibrium which are quite significant, even at heights as low as 200 Km. (J. V. Evans (1967)). The recent measurements by the IMP II satellite by G. P. Serbu and E. J. Maier (1966a, b) on electron and ion temperatures in the outer magnetosphere revealed a steep increase of both temperatures with height. Fig. 7 gives the results of these measurements together with the profiles of the neutral gas temperatures in the thermosphere. The latter are given for three different levels of solar activity. The diurnal average temperatures only are plotted.

The solid curve in the upper right part of Fig. 7 has been calculated for ionic heat conduction perpendicular to the magnetic field, in a fully stable plasma, assuming a heat reservoir at a height of 5.10^4 Km with a temperature of 7.10^4 ^oK. This is thought to be provided by the continuous flow of the solar wind, the temperature of which is in the order of 7.10^4 ^oK. A sufficiently good agreement is obtained if a temperature gradient of 2.65 $^oK/km$ is assumed at the upper boundary at a height of 5.10^4 km. Thus the observed ion temperatures could be considered to be compatible with this kind of heat conduction. The heat flow associated with it, however, would be extremely small, in the order of 5.10^{-15} erg/cm^2 sec. This, indeed, would provide a perfect insulation of the thermosphere.

Since the plasma of the magnetosphere, however, is far from being in a stable state, we can expect a heat flow which is many orders of magnitude larger than the figure given above. As H. G. Mayr and H. Volland (1967) argue, it might even reach an order of magnitude which is comparable with the conductivity parallel to the magnetic field lines. Under those circumstances the calculations for a stable plasma would no longer have any significance. But also the insulation of the thermosphere would be considerably less effective. This might then lead to a non-zero temperature gradient in the lower exosphere and upper thermosphere. Since temperatures, so far, cannot be measured directly in the lower exosphere (500 to 1000 Km) it is very important to derive temperatures from height profiles of the different atomic constituents, in particular, of oxygen and helium in the height range up to 1000 Km. A further interesting feature of the temperature structure is the rather steep increase of the ion temperatures at heights above 400 Km as it was revealed by the Thomson scatter technique (J. V. Evans 1967). These data could have an important bearing on whether the structure of the neutral gas in the lower exosphere is isothermal. Evans explains the ion and electron temperature profile by heating due to fast photoelectrons which are being produced in the thermosphere in the absorption process of solar XUV-radiation. The basic argument for the photoelectron heating are the observed seasonal variations in the ion and electron temperatures.

6. Conclusions

In this paper we have attempted to give an account of our present understanding of the thermal structure of the upper atmosphere in the range from 120 Km to about 1000 Km and of its key-feature, the diurnal variation. The basic problem how to explain the density and temperature maximum at 1400 hours local time is still unsettled; The open questions are:

1. Is the solar XUV flux sufficient to provide the entire energy for the heating of the thermosphere, even for the highest level of solar activity?
2. If so, can then the horizontal advection set up by the pressure gradients around the atmospheric bulge provide enough horizontal energy transport in order to account for the 1400 hours maximum of the density in the upper thermosphere?
3. How large is the heat flux which arrives at the upper level of the thermosphere (thermopause) from the solar wind through the magnetosphere under geomagnetically quiet conditions? Is the heat flux large enough to distort the isothermal structure of the upper thermosphere and lower exosphere? If so, does the heat flux have a significant variation with the orientation of the earth, in particular with local time?

These 3 complexes of questions must be answered before a sufficient understanding of the physical behavior of the thermosphere can be reached.

REFERENCES

Bates, D. R., 1951: The temperature of the upper atmosphere. Proc. Phys. Soc. London, 64B, 809-921.

Chandra, C., 1963: Electron Density Distribution in the Upper F-region. J. Geophys. Res. 68, 1937-1942.

Chapman, S., 1956: The electrical conductivity of the ionosphere. Nuovo Cimento 4, Suppl., 1385-1412.

Cook, G.E. and Scott, D.W., 1966: Exospheric densities near solar minimum derived from the orbit of Echo 2. Planet. Space Sci., 14, 1149-1165.

COSPAR Working Group IV, 1965: CIRA 1965, Cospar International Reference Atmosphere 1965. North Holland Publ. Co., Amsterdam.

Evans, J.V., 1967: The heating of the protonosphere. COSPAR Symposium, London July, 1967, preprint, 7 pg.

Geisler, J.E., 1966: Atmospheric winds in the middle latitude F-region. J. Atmosph. Terr. Phys. 28, 703-720.

Geisler, J.E., 1967: A numerical study of the wind system in the middle thermosphere. Transactions AGU. 48, 104.

Harris, I., 1966: Horizontal energy transport in the thermosphere. Transactions AGU 47, 459.

Harris, I. and Priester, W., 1962a: Time-dependent structure of the upper atmosphere. J. Atmosph. Sci. 19, 286-301.

Harris, I. and Priester, W., 1962b: Theoretical model for the solar-cycle variations of the upper atmosphere. J. Geophys. Res. 67, 4585-4591.

Harris, I. and Priester, W., 1963a: Heating of the upper atmosphere. Space Res. III (W. Priester ed.) 53-75.

Harris, I. and Priester, W., 1963b: Relation between theoretical and observational models of the upper atmosphere. J. Geophys. Res. 68, 5891-5894.

Harris, I. and Priester, W., 1965: Of the diurnal variation of the upper atmosphere. J. Atmospheric Sci. 22, 3-10.

REFERENCES (CONT"D)

Hinteregger, H.E., 1961: Preliminary data on solar extreme ultraviolet radiation in the upper atmosphere. J. Geophys. Res. 66, 2367-2380.

Hinteregger, H.E., Hall, L.A. and Schmidtke, G., 1965: Solar XUV radiation and neutral particle distribution in July 1963 thermosphere. Space Res. V (D.G. King-Hele et. al., eds.), 1175-1190.

Jacchia, L.G., 1959: Solar effects on the acceleration of artificial satellites. Smithsonian Astrophys. Obs. Spec. Rep. No. 29, 15 pg.

Jacchia, L.G., 1967: The structure of the thermosphere and its variations. Proc. IQSY/COSPAR Symposium, London, July 1967.

Jacchia, L.G. and Briggs, R.E., 1958: Orbital acceleration of satellite 1958 beta two. Smithsonian Contr. Astrophys. 6, 13-19.

Jacchia, L. G. and Slowey, J., 1963: Atmospheric heating of the auroral zones: A preliminary analysis of the atmospheric drag of Injun III satellite. Smithsonian Astrophys. Obs. Spec. Rep. 136.

Jacchia, L.G. and Slowey, J., 1967: Diurnal and seasonal-latitudinal variations in the upper atmosphere. Smithsonian Astrophys. Obs. Spec. Rep. No. 242, 32 pg.

Jastrow, R. and Kyle, L., 1961: The earth atmosphere. Handbook of Astrononautical Engineering (H.H. Koelle ed.) Chapter 2, pp 2-13, New York 1961.

Johnson, F.S., 1956: Temperature distribution of the ionosphere under control of thermal conductivity. J. Geophys. Res. 61, 71-76.

Keating, G.M. and Prior, E.J., 1967: The winter helium bulge. Proc. IQSY/COSPAR Symposium, London July 1967.

Kohl, H., 1967: Atmospheric winds in the ionosphere. Proc. IQSY/COSPAR Symposium London, July 1967.

Kohl, H. and King, J.W., 1966: Atmospheric winds between 100 and 700 km and their effects on the ionosphere. Rep. Radio and Space Res. Station, Slough.

REFERENCES (CONT"D)

Lindzen, R.S., 1966: Diurnal velocity oscillations in the thermosphere. J. Geophys. Res. 71, 815-820.

Lindzen, R.S., 1967: Reconsideration of diurnal velocity oscillation in the thermosphere. J. Geophys. Res. 72, 1591-1598.

Mahoney, J.R., 1966: A study of energy sources for the thermosphere. Mass. Inst. Technology, Dept. Meteorology Rep. No. 17, MIT-2241-16, 218 pg.

Mauersberger, K., Mueller, D., Offermann, D. and von Zahn, U., 1967: A mass spectrometric determination of the neutral constituents in the lower thermosphere above Sardinia. J. Geophys. Res. (in press).

Mayr, H.G. and Volland, H., 1967: On the magnetospheric temperature distribution. Goddard Space Flight Center, Rep. X-621-67-291, 17 pg.

Newton, G., Pelz, D. and Volland, H., 1967: Direct in situ observations of wave propagation in the neutral thermosphere. submitted to J. Geophys. Res.

Nicolet, M., 1961: Structure of the thermosphere. Planet. Space Sci. 5, 1-32.

Priester, W., 1959: Sonnenaktivität und abbremsung der Erdsatelliten. Naturwiss. 46, 197-198.

Priester, W. and Martin, H.A., 1960: Solare und tageszeitliche Effekte in der Hochatmosphaere aus Beobachtungen Kuenstlicher Erdsatelliten. Mitt. Univ. Sternwarte Bonn, No. 29, 53 pg.

Priester, W., Roemer, M. and Volland, H., 1967: The physical behavior of the upper atmosphere deduced from satellite drag data. Space Sci. Rev. 6, 707-780.

Serbu, G.P. and Maier, E.J.R., 1966a: Low energy electrons measured on IMP II. J. Geophys. Res. 71, 3755-3766.

Serbu, G.P. and Maier, E.J.R., 1966b: Thermal plasma measurements within the magnetosphere. Goddard Space Flight Center. Rep. X-615-66-328.

Tsuda, T., 1967: Effective viscosity of a streaming collision-free plasma in a weakly turbulent magnetic field. Transactions AGU 48, 61.

REFERENCES (CONT"D)

Waldmeier M. and Mueller, H., 1950: Die Sonnenstrahlung im Gebiet von λ = 10 cm. Zeitschr. f. Astrophysik 27, 58-72.

Wyatt, S.P., 1959: Solar effect in the motion of Vanguard. Nature 184 Suppl., 351-352.

FIGURE CAPTIONS

Fig. 1: Densities at a height of 250 km above sea level derived from Injun III by Jacchia and Slowey (1963) for the time interval from December 15, 1962 through June 1963. The data are plotted as a function of local time of the perigee. The corresponding dates are given at the top, also as MJD (Modified Julian Dates). For comparison, the geomagnetic indices A_p and the solar 10.7 cm flux F are presented. The numbers on the densities indicate the geographic latitudes of the perigree. The curves represent the Harris-Priester models S = 90 and S = 100.

Fig. 2: Comparison of CIRA Model densities with data derived from satellite drag measurements (from CIRA, 1965). The models are for high solar activity (Model 7, $\overline{F}$ = 200) and very low solar activity (Model 2, $\overline{F}$ = 75). The observational data are the Bonn model 1961 for $\overline{F}$ = 200 and the data derived by Jacchia and Slowey for March 1963 corresponding to $\overline{F}$= 78 and 04 hours local time from the 5 satellites Injun III, Explorer I, Explorer VIII, Vanguard II and Explorer IX. The maximum and minimum exospheric temperatures are stated on the right.

Fig. 3: Variation of atmospheric density at a height of 1130 Km derived from Echo II by G. E. Cook and D. W. Scott (1966). The densities display a pronounced semi-annual variation.

FIGURE CAPTIONS (CONT"D)

Fig. 4: Diurnal variation of the temperature at the thermopause (500 km). The abscissa is the local time t. The observed temperature T_M (dashed-dotted curve, inferred from density measurements) is compared with calculated temperature variations. The dashed curve (T_{EUV}) is calculated under the assumption of heating by the absorption of solar XUV-radiation and no horizontal advection. The solid curve (T_C) is obtained when the effect of horizontal advection in the equatorial plane is included.

Fig. 5: The heat source functions, integrated over the entire height range, as function of local time t. The integrals I correspond to that portion of the incoming solar energy which is converted into heat in the thermosphere. The physical interpretation of the 4 curves is explained in the text.

Fig. 6: The wind velocities in the equatorial plane for 4 different heights from 150 to 400 km as function of local time t. These high velocities were obtained when the ion drag was considerably suppressed (see text).

Fig. 7: The temperature profile of the earth's outer atmosphere. In the height range $z < 10^3$ km the neutral gas temperatures (diurnal averages) are given for three levels of solar activity $\bar{F}$ = 275, 150 and 65. In the upper right the electron temperatures (circles) and ion temperatures (circles with + signs inside) as measured by Serbu and Maier (1966a,b) are given.

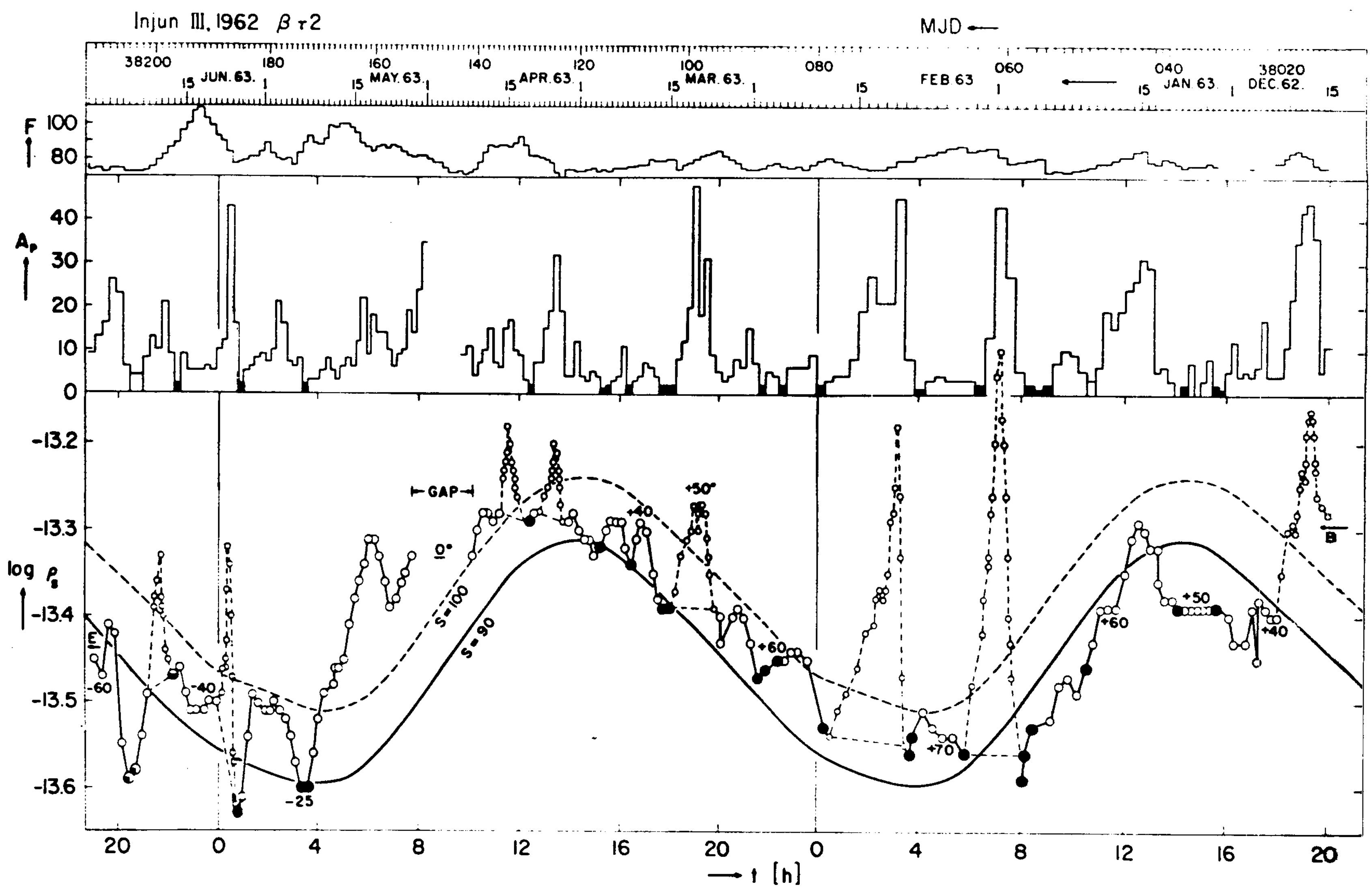

Injun III, 1962 β τ2
MJD ⟵
38200
15 JUN. 63.
180
160
15 MAY. 63.
140
15 APR. 63.
120
100
15 MAR. 63.
080
15
FEB 63
060
040
15 JAN 63.
38020
DEC. 62.
15
F
100
80
A_p
40
30
20
10
0
log ρ_s
-13.2
-13.3
-13.4
-13.5
-13.6
⊢ GAP ⊣
0°
+50°
+40
+60
+70
+50
-60
-40
-25
S = 100
S = 90
B
E
20
0
4
8
12
16
20
0
4
8
12
16
20
⟶ t [h]

fig 1

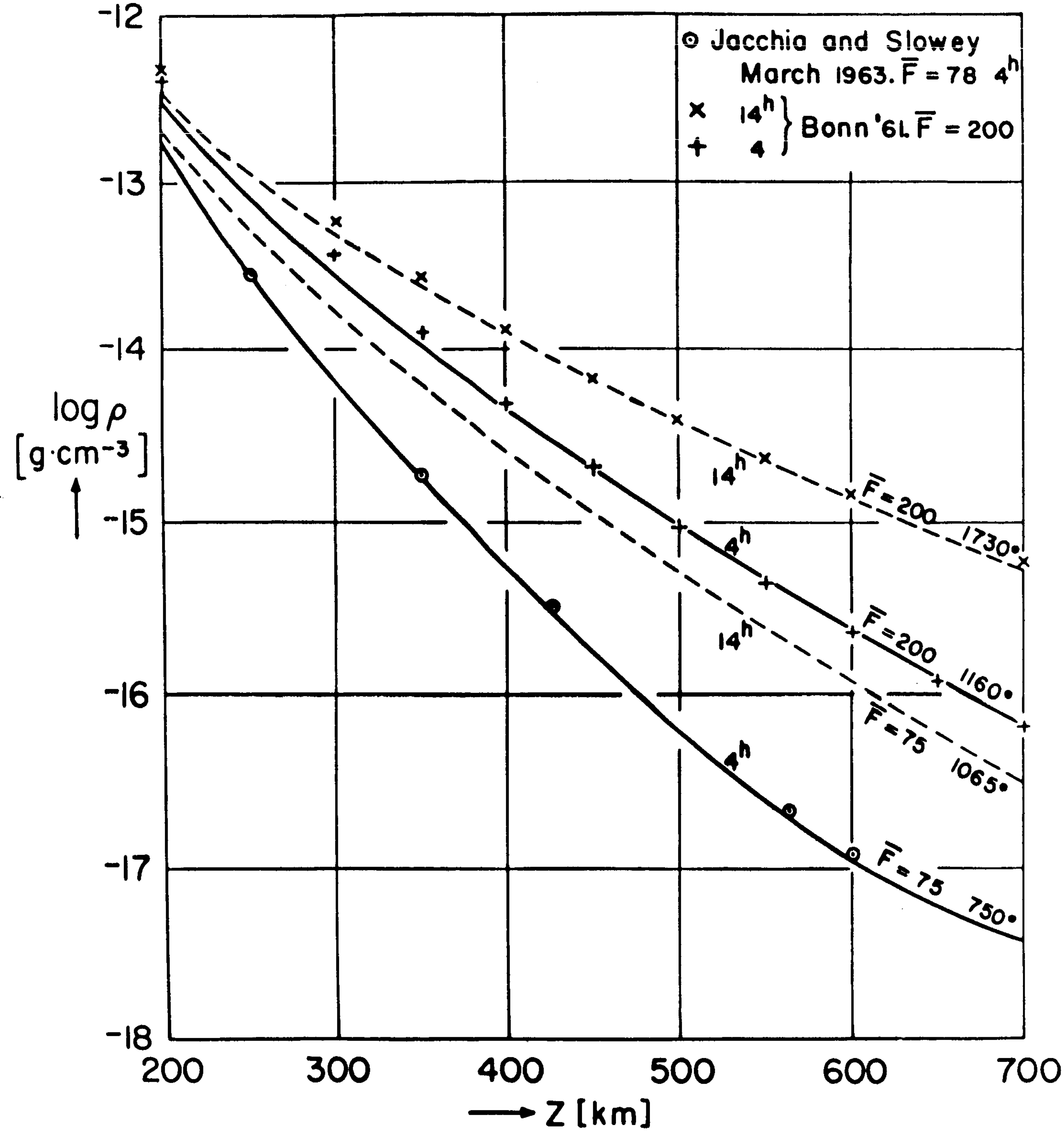

⊙ Jacchia and Slowey
March 1963. $\overline{F}$ = 78 4^h
× 14^h
+ 4
Bonn '61. $\overline{F}$ = 200
-12
-13
-14
-15
-16
-17
-18
log ρ
[g·cm⁻³]
200
300
400
500
600
700
Z [km]
14^h
$\overline{F}$ = 200
1730°
4^h
$\overline{F}$ = 200
1160°
14^h
$\overline{F}$ = 75
1065°
4^h
$\overline{F}$ = 75
750°

fig 2

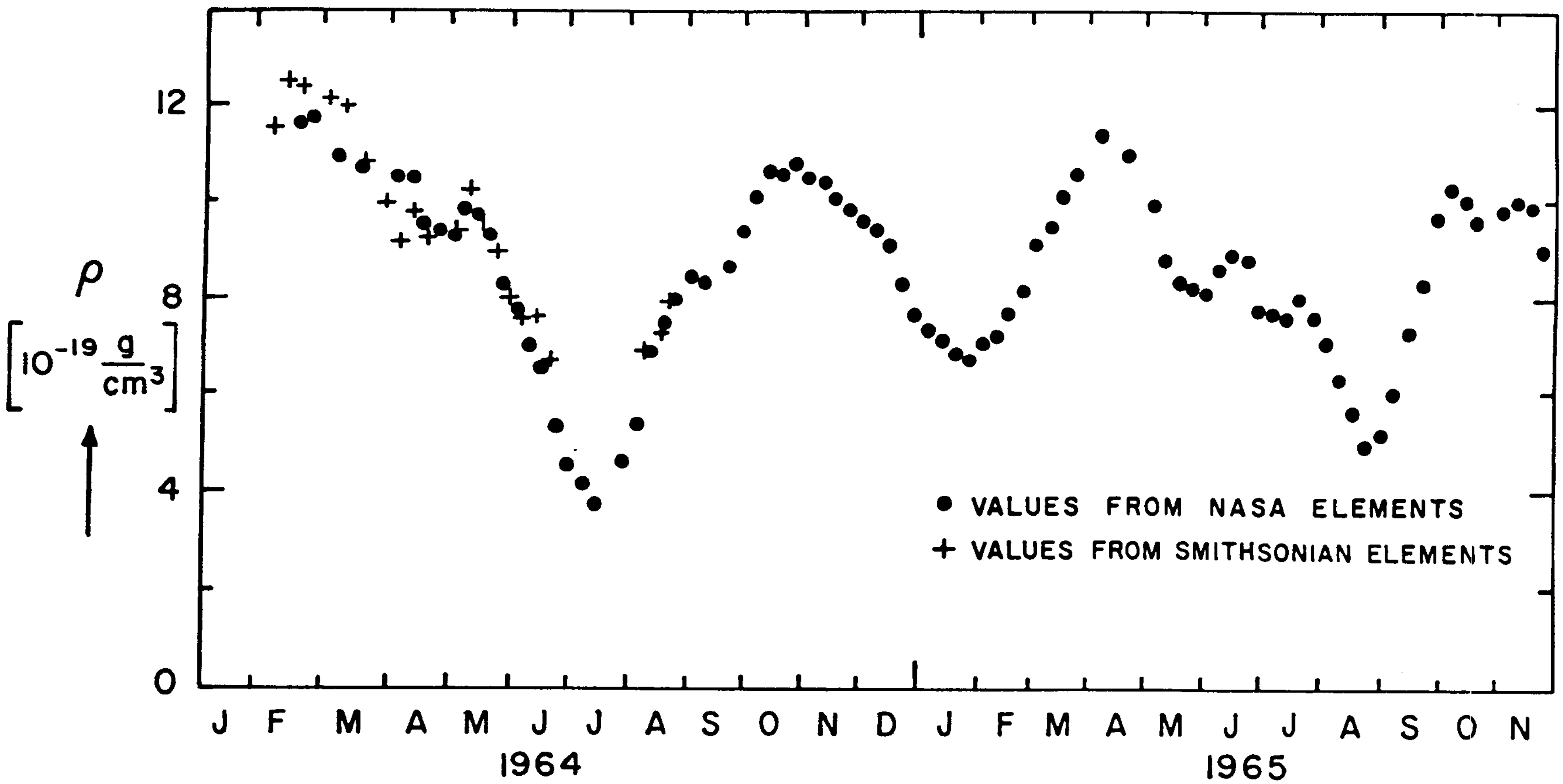
ρ
[10^{-19} g/cm³]
12
8
4
0
J F M A M J J A S O N D J F M A M J J A S O N
1964
1965
● VALUES FROM NASA ELEMENTS
+ VALUES FROM SMITHSONIAN ELEMENTS

fig 3

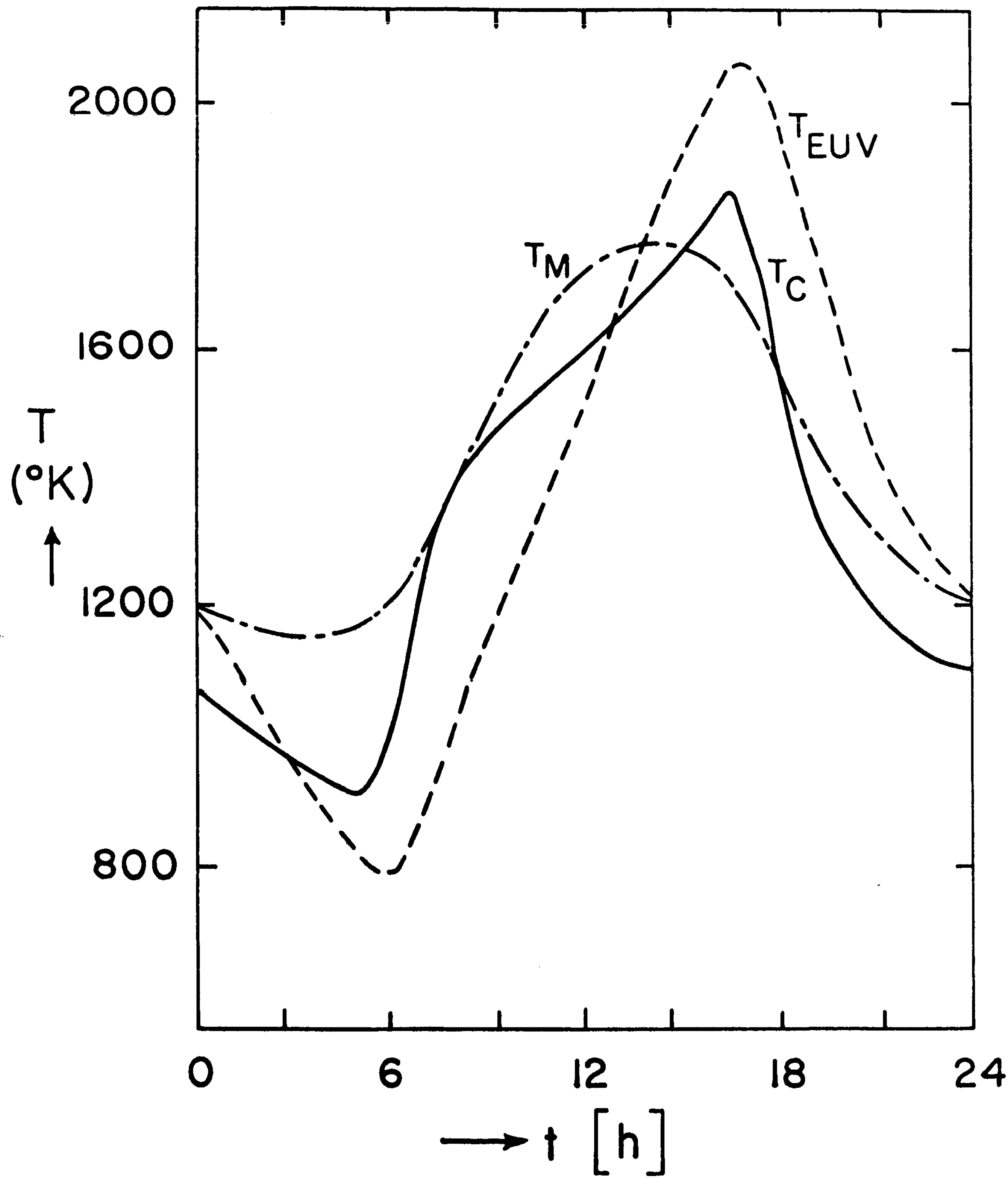

fig 4

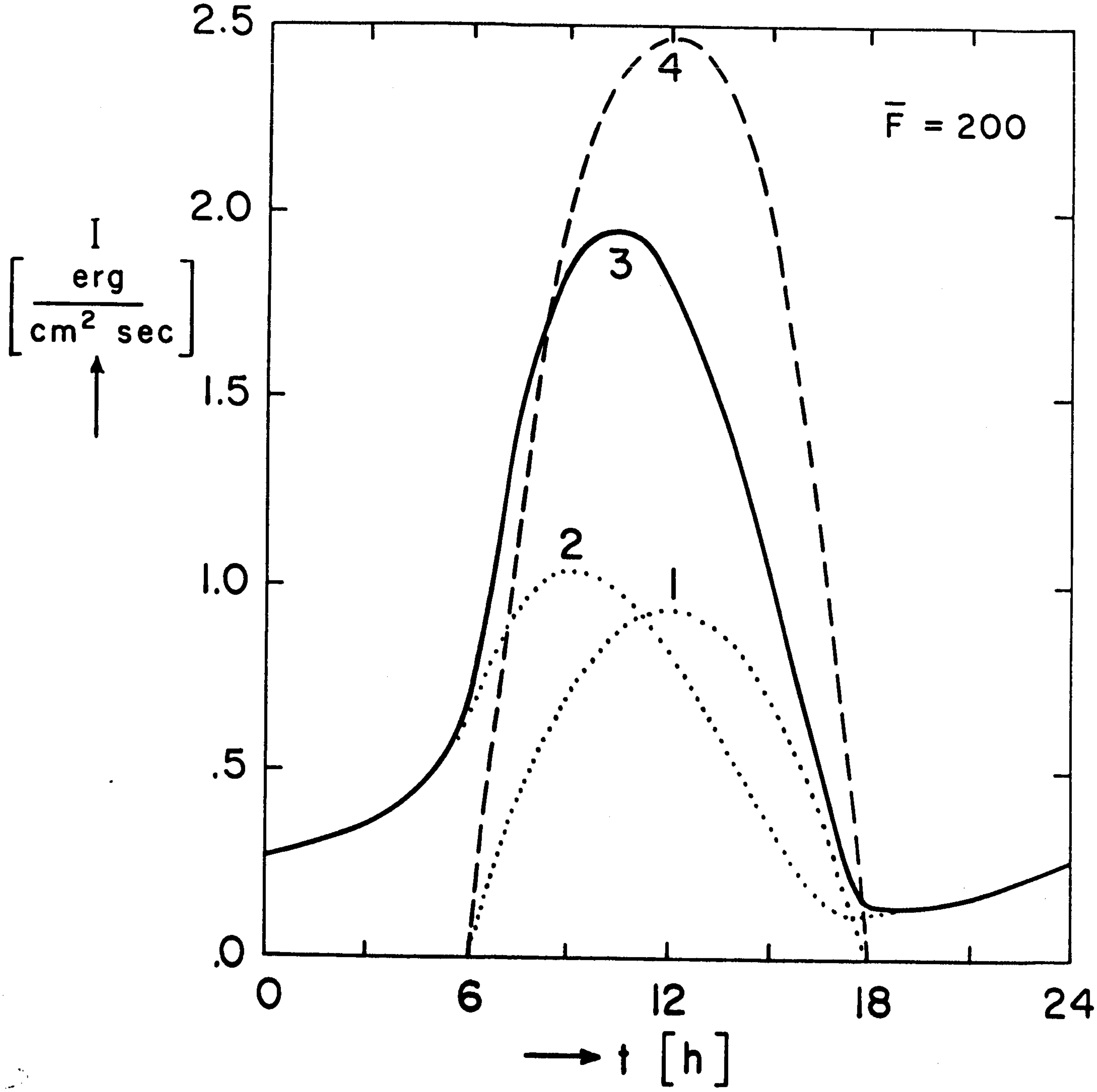

fig 5

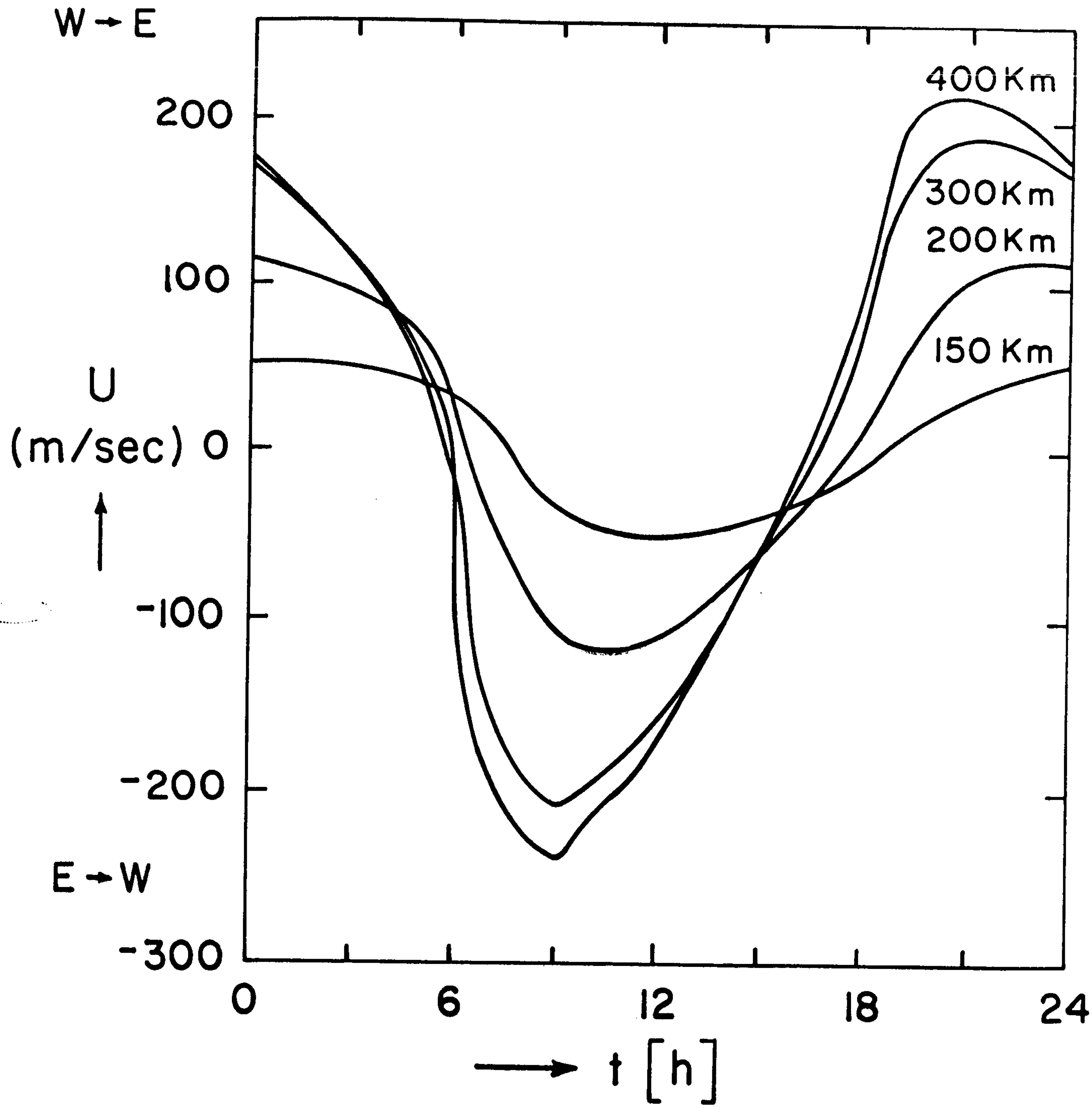

W → E
200
100
U
(m/sec) 0
-100
-200
E → W
-300
0
6
12
18
24
t [h]
400 Km
300 Km
200 Km
150 Km

fig 6

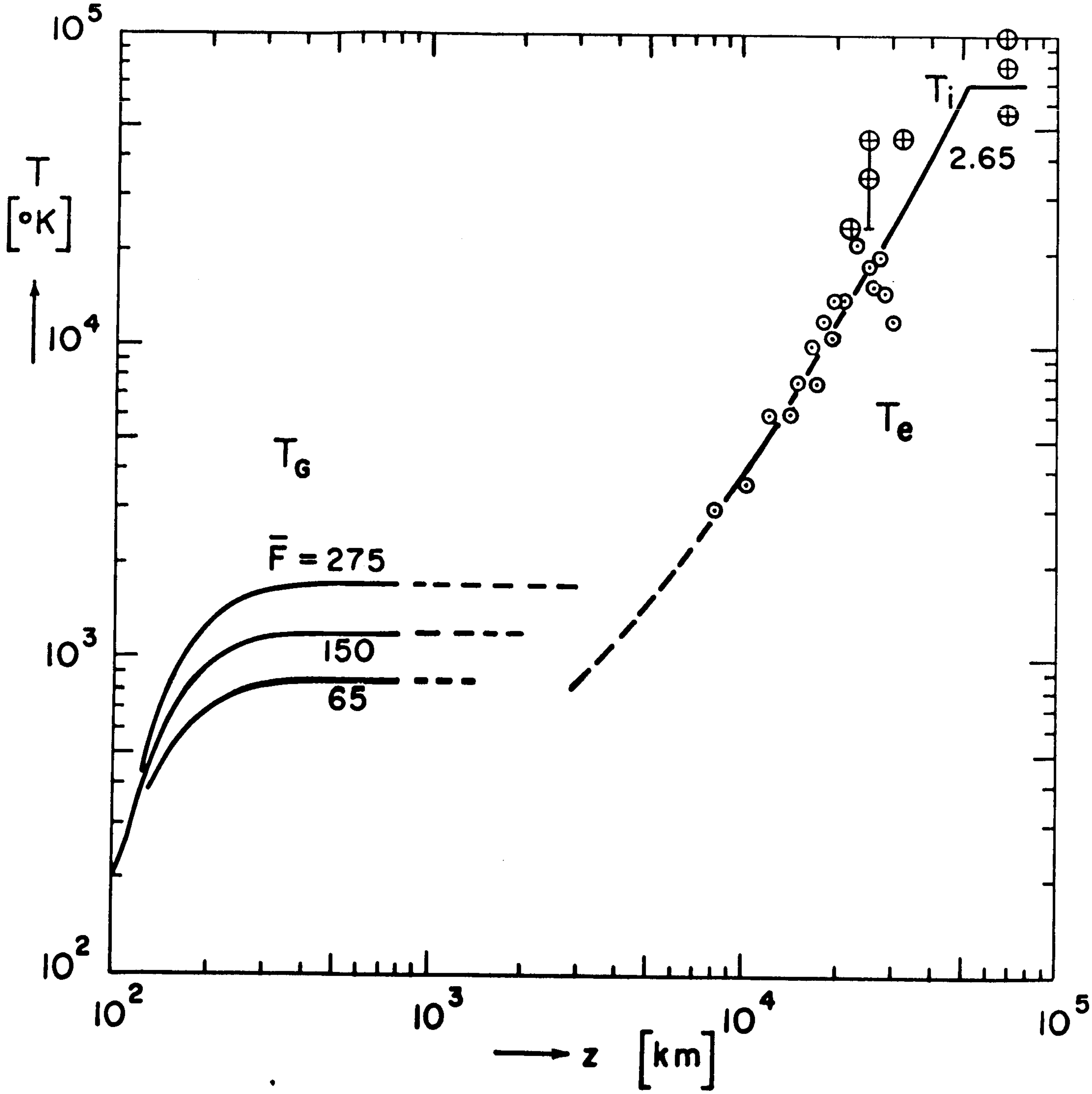

T [°K]
10^5
10^4
10^3
10^2
T_i
2.65
T_e
T_G
$\bar{F} = 275$
150
65
10^2
10^3
10^4
10^5
z [km]

fig 7